Cell Reports

Report

Therapeutic Response to Non-genotoxic Activation of p53 by Nutlin3a Is Driven by PUMA-Mediated Apoptosis in Lymphoma Cells

Graphical Abstract

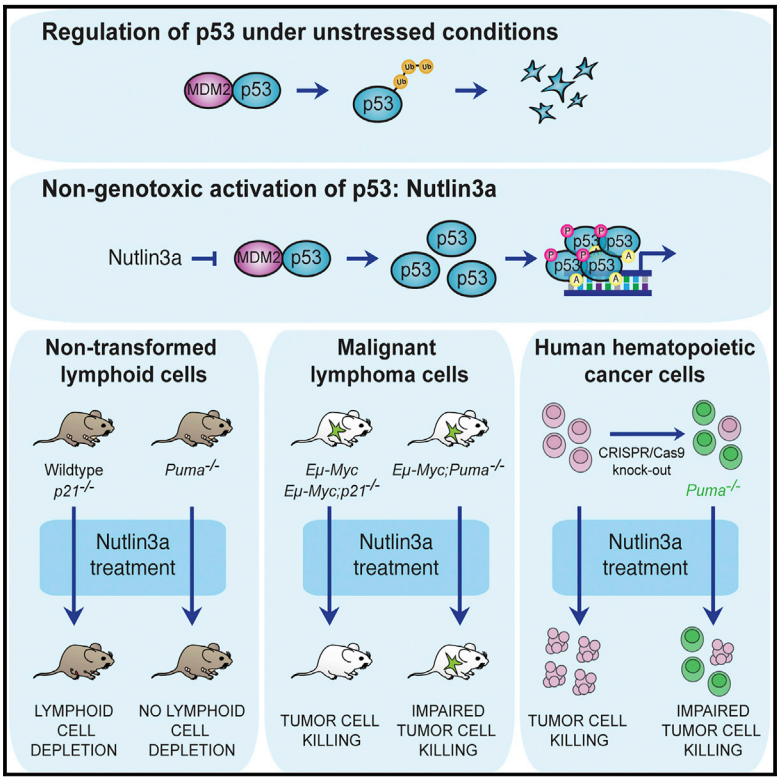

Highlights

- Nutlin3a induces p53 activation and target gene expression in mouse lymphoid cells
- Loss of PUMA, but not loss of p21, impairs treatment responses to Nutlin3a
- Malignant lymphoma cells are more sensitive to Nutlin3a than normal lymphocytes
- PUMA is critical for Nutlin3a-induced killing of MYC-driven lymphoma cells

Authors

Liz J. Valente, Brandon J. Aubrey, Marco J. Herold, ..., David C.S. Huang, Lyubomir T. Vassilev, Andreas Strasser

Correspondence

strasser@wehi.edu.au

In Brief

Using transgenic and gene-targeted mice, Valente et al. show that PUMA-mediated apoptosis, and not cell-cycle arrest or senescence mediated by p21, is critical for the therapeutic responses of both non-transformed and malignant lymphoid cells to the p53-activating compound Nutlin3a.

Valente et al., 2016, Cell Reports *14*, 1858–1866
March 1, 2016 ©2016 The Authors
http://dx.doi.org/10.1016/j.celrep.2016.01.059

CellPress

OPEN ACCESS
CellPress

Cell Reports
Report

Therapeutic Response to Non-genotoxic Activation of p53 by Nutlin3a Is Driven by PUMA-Mediated Apoptosis in Lymphoma Cells

Liz J. Valente,[1,2,7] Brandon J. Aubrey,[1,2,3] Marco J. Herold,[1,2] Gemma L. Kelly,[1,2] Lina Happo,[1,2] Clare L. Scott,[1,2] Andrea Newbold,[4,5] Ricky W. Johnstone,[4,5] David C.S. Huang,[1,2] Lyubomir T. Vassilev,[6,8] and Andreas Strasser[1,2,*]

[1]The Walter and Eliza Hall Institute of Medical Research, Melbourne, VIC 3052, Australia
[2]Department of Medical Biology, University of Melbourne, Melbourne, VIC 3052, Australia
[3]Department of Clinical Haematology and Bone Marrow Transplant Service, The Royal Melbourne Hospital, Parkville, VIC 3050, Australia
[4]Cancer Therapeutics Program, Peter MacCallum Cancer Centre, Melbourne, VIC 3002, Australia
[5]Sir Peter MacCallum Department of Oncology, University of Melbourne, Melbourne, VIC 3002, Australia
[6]Discovery Oncology, Hoffmann-La Roche Inc., Nutley, NJ 07110, USA
[7]Present address: Division of Radiation and Cancer Biology, Department of Radiation Oncology, Stanford University School of Medicine, Stanford, CA 94305, USA
[8]Present address: EMD Serono Research and Development Institute, Billerica, MA 01821, USA
*Correspondence: strasser@wehi.edu.au
http://dx.doi.org/10.1016/j.celrep.2016.01.059
This is an open access article under the CC BY-NC-ND license (http://creativecommons.org/licenses/by-nc-nd/4.0/).

SUMMARY

Nutlin3a is a small-molecule antagonist of MDM2 that promotes non-genotoxic activation of p53 through p53 protein stabilization and transactivation of p53 target genes. Nutlin3a is the forerunner of a class of cancer therapeutics that have reached clinical trials. Using transgenic and gene-targeted mouse models lacking the critical p53 target genes, *p21*, *Puma*, and *Noxa*, we found that only loss of PUMA conferred profound protection against Nutlin3a-induced killing in both non-transformed lymphoid cells and *Eμ-Myc* lymphomas in vitro and in vivo. CRISPR/Cas9-mediated targeting of the *PUMA* gene rendered human hematopoietic cancer cell lines markedly resistant to Nutlin3a-induced cell death. These results demonstrate that PUMA-mediated apoptosis, but not p21-mediated cell-cycle arrest or senescence, is a critical determinant of the therapeutic response to non-genotoxic p53 activation by Nutlin3a. Importantly, in human cancer, PUMA expression may predict patient responses to treatment with MDM2 antagonists.

INTRODUCTION

The tumor suppressor p53 is a transcription factor capable of modulating activity in a wide range of cellular processes through its regulation of recognized target genes. p53 is activated post-translationally in response to diverse cellular stressors, such as DNA damage, hypoxia, and activation of oncogenic proteins (Riley et al., 2008). In unstressed cells, the levels of p53 protein are kept low as a result of an auto-regulatory negative-feedback loop involving the E3 ubiquitin ligase, MDM2, which targets p53 for proteasomal degradation (Vogelstein et al., 2000).

Many frequently used anti-cancer therapeutics kill tumor cells by inducing DNA damage, which activates p53. This, in turn, causes the induction of downstream target genes, with consequent activation of effector processes that limit tumor expansion by inducing cell-cycle arrest, senescence, or death. Studies utilizing gene-targeted mice have identified the downstream effectors critical for the induction of these processes. The cyclin-dependent kinase inhibitor (CDKI) p21 is critical for p53-mediated G1/S cell-cycle arrest and senescence (Brugarolas et al., 1995; Chang et al., 1999; Deng et al., 1995), whereas the BH3-only proteins PUMA and (to a lesser extent) NOXA are required for the induction of apoptosis (Jeffers et al., 2003; Oda et al., 2000; Shibue et al., 2003; Villunger et al., 2003).

While ~50% of all human cancers bear mutations in *p53*, many other cancers utilize indirect mechanisms to silence p53 tumor growth suppressive pathways, such as MDM2 gene amplification (Freedman et al., 1999; Momand et al., 1998). Thus, targeting the MDM2-p53 interaction constitutes an exciting approach for the design of non-genotoxic anti-cancer therapeutics. Nutlin3a, is the forerunner of this class of compounds. By binding within the p53 interaction site on MDM2, Nutlin3a inhibits p53 ubiquitination and proteasomal degradation, thereby promoting stabilization and activation of p53, with consequent induction of downstream effector processes (Efeyan et al., 2007; Vassilev et al., 2004). While genetic studies revealed the processes mediating tumor regression in response to acute p53 restoration (Martins et al., 2006; Ventura et al., 2007; Xue et al., 2007), and microarray gene expression analyses have provided insight into which target genes are expressed after Nutlin3a treatment (Tovar et al., 2006; Vassilev et al., 2004), it remains unclear which p53 target genes are essential for Nutlin3a's therapeutic activity.

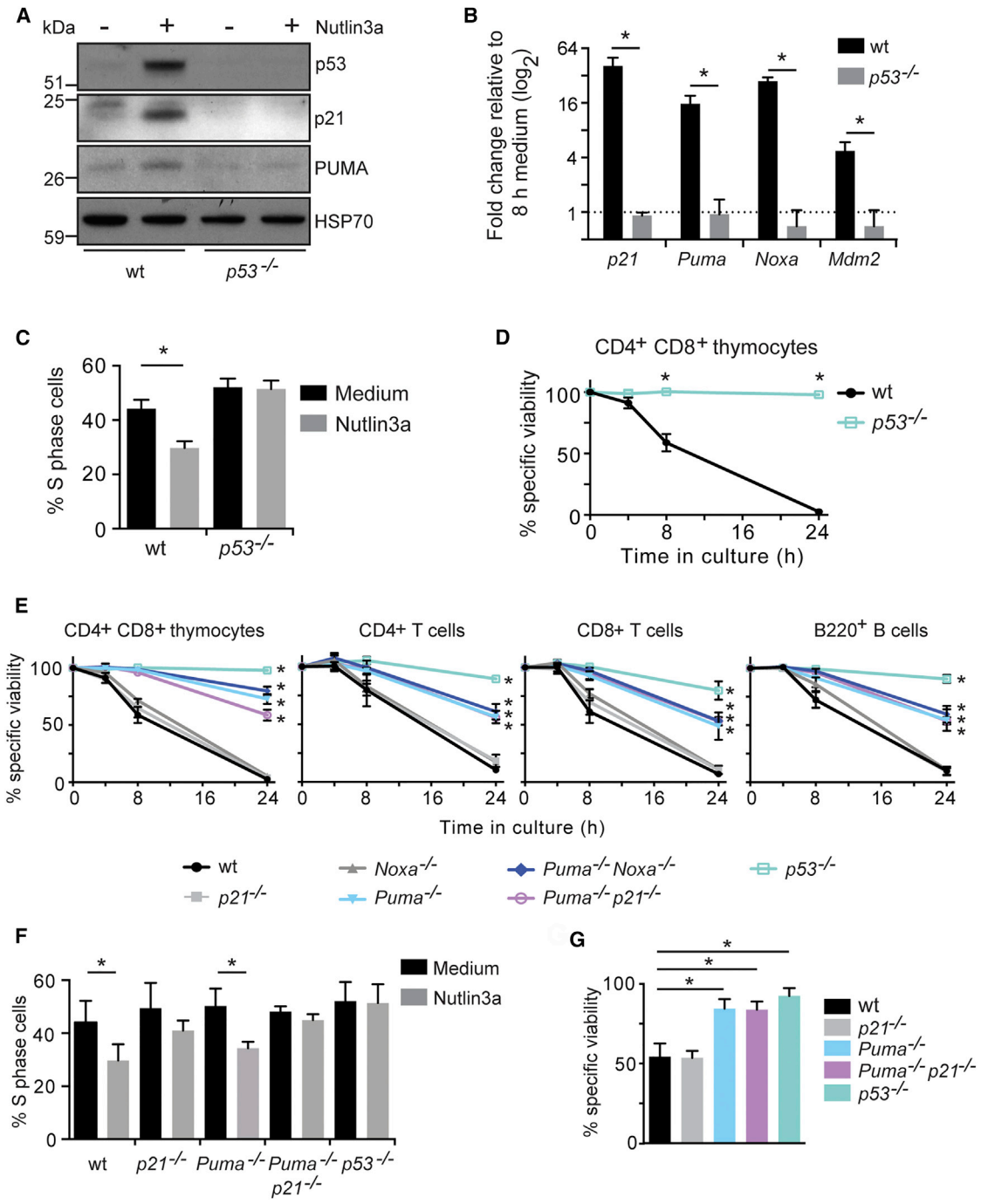

Figure 1. PUMA, but Not p21, Is Critical for Nutlin3a-Induced, p53-Dependent Killing of Non-transformed Quiescent and Proliferating Lymphoid Cells In Vitro

(A) WT and $p53^{-/-}$ thymocytes were treated with 20 μM Nutlin3a (or DMSO control) for 8 hr (in the presence of QVD-OPH (25 μM)) prior to analysis for p53, p21, and PUMA protein expression by western blotting.

(B) Real-time PCR analysis for p53 target gene expression in WT and $p53^{-/-}$ thymocytes treated with 20 μM Nutlin3a for 8 hr (or DMSO control) in the presence of QVD-OPH.

(C) Cell-cycle analysis after 12 hr of Nutlin3a treatment in mitogen-stimulated proliferating T lymphocytes in vitro.

(D and E) Cell-survival analysis of sorted primary $CD4^+CD8^+$ thymocytes (D and E) and $CD4^+$ T cells, $CD8^+$ T cells, or $B220^+$ B cells (E) (from lymph nodes) of mice of the indicated genotypes (Figure S1).

(legend continued on next page)

We utilized gene-targeted mice lacking critical p53 target genes, or human hematopoietic cancer cell lines targeted with CRISPR/Cas9, to define the pathways activated by p53 that are critical for Nutlin3a's therapeutic effects. Our results demonstrate that apoptotic pathways initiated by the BH3-only protein PUMA, but not anti-proliferative pathways mediated by the CDKI p21, are responsible for Nutlin3a's therapeutic activity in lymphoid malignancies.

RESULTS AND DISCUSSION

Nutlin3a Activates p53 Target Gene Expression and Causes Cell-Cycle Arrest and Apoptosis in Non-transformed Mouse Lymphoid Cells In Vitro

First, we assessed the impact of Nutlin3a on non-transformed cells. Accumulation of p53 protein and the p53 targets, PUMA and p21, was readily detectable at the protein (Figure 1A) and mRNA level (*Puma*, *Noxa*, *p21*, and *Mdm2*; Figure 1B) in wild-type (WT) but not $p53^{-/-}$ thymocytes after 8-hr treatment. Nutlin3a treatment promoted p53-dependent G1/S-phase cell-cycle arrest in mitogen-stimulated proliferating WT T cells, evidenced by an ~50% decrease in the S-phase population (Figure 1C). In $CD4^{+}CD8^{+}$ WT thymocytes (isolated through fluorescence-activated cell sorting [FACS]), Nutlin3a promoted apoptosis with >90% cell death within 24 hr, whereas $p53^{-/-}$ thymocytes were protected (Figure 1D). Lymphocytes overexpressing the pro-survival gene *BCL2* (Ogilvy et al., 1999) were resistant to Nutlin3a, indicating that death was mediated by the intrinsic apoptotic pathway (Figure S1). At 24 hr, a small subset (~5%–20%) of $p53^{-/-}$ cells had undergone apoptosis, whereas *vav-Bcl2* lymphocytes remained completely protected (Figure S1). This finding is, perhaps, explained by previous studies reporting that Nutlin3a can induce a p53-independent genotoxic response in cancer cells, evidenced by the appearance of γH2AX foci (a marker of double-stranded DNA [dsDNA] breaks), albeit to a much lesser extent than that induced by DNA-damage-inducing drugs (Rigatti et al., 2012; Valentine et al., 2011; Verma et al., 2010).

Nutlin3a-Mediated Killing of Non-transformed Mouse Lymphoid Cells In Vitro Requires PUMA, but Not p21

Next, we analyzed lymphoid cells from a panel of gene-targeted mice lacking single or multiple downstream p53 effectors. Doses of 4 μM Nutlin3a induced complete killing of diverse lymphoid cell populations from WT, $p21^{-/-}$, and $Noxa^{-/-}$ mice, but not $p53^{-/-}$ mice, within 24 hr (Figure 1E). $Puma^{-/-}$ cells exhibited comparable resistance to $p53^{-/-}$ cells after 8 hr of treatment (Figure 1E). Interestingly, at 24 hr, significantly lower protection was seen in the $Puma^{-/-}$ cells (albeit still much higher than in WT cells) (Figure 1E).

Analysis of lymphocytes from $Puma^{-/-}Noxa^{-/-}$ mice showed that loss of NOXA did not further enhance the resistance to Nutlin3a afforded by the loss of PUMA. This contrasts with previous studies in which NOXA was shown to contribute, albeit to a lesser extent, to p53- and p63-mediated apoptosis induced by γ-irradiation or DNA-damaging anti-cancer therapeutics (Kerr et al., 2012; Michalak et al., 2008; Villunger et al., 2003) (Figure 1E). Lymphoid cells from $Puma^{-/-}p21^{-/-}$ mice exhibited resistance to Nutlin3a comparable to that of the $Puma^{-/-}$ cells, demonstrating that loss of p21 cannot provide a protective effect against Nutlin3a-induced cell killing, even in the context of PUMA deficiency (Figure 1E).

In proliferating T cells, the loss of p21 significantly reduced Nutlin3a-induced cell-cycle arrest, comparable to the reduction seen in $p53^{-/-}$ T lymphoblasts, but PUMA deficiency had no such impact (Figures 1E and 1F). Notably, although $p21^{-/-}$ T lymphoblasts did not undergo cell-cycle arrest, they remained normally sensitive to Nutlin3a-induced killing. In contrast, T lymphoblasts lacking PUMA or p53 were almost entirely resistant to Nutlin3a-induced killing (Figure 1G).

Our finding that loss of p21 fails to impact Nutlin3a-induced apoptosis is in contrast to previous studies, which suggested a role for p21 in inhibiting p53-mediated apoptosis (induced by DNA-damage-inducing compounds) (Gartel and Tyner, 2002; Jänicke et al., 2007; Tian et al., 2000), but they are consistent with a report that dysregulated expression of p21 (overexpression or knockdown) had no impact on Nutlin3a-induced apoptosis in human cancer-derived cell lines. This suggests that p21's ability to modulate p53-mediated apoptosis may depend on the presence of DNA damage (Xia et al., 2011).

Loss of PUMA, but Not Loss of p21, Protects Non-transformed Mouse Lymphoid Cells against Nutlin3a-Induced Killing In Vivo

Next, we treated mice lacking various p53 downstream effector genes with Nutlin3a. Nutlin3a was shown to be well tolerated in mice, with no weight loss or gross abnormalities (beyond lymphocyte depletion) observed after treatment with 200 mg/kg Nutlin3a for 20 days (Tovar et al., 2006; Vassilev et al., 2004). Similarly, we observed no evidence of weight loss, thrombocytopenia, or anemia in our Nutlin3a-treated mice (Figure S2A).

In response to Nutlin3a treatment, upregulation of the p53 target genes *p21*, *Puma*, and *Noxa* was readily observed in thymic and lymph node extracts from WT, but not $p53^{-/-}$, mice (Figure 2A; Figure S2B). In WT mice, Nutlin3a treatment reduced thymocyte numbers by ~90% (Figure 2B) and mature T lymphocyte numbers in the lymph nodes by 50%–60% (Figure S2C). Loss of p21 did not protect against Nutlin3a in vivo, with an ~65% reduction of thymocytes recorded in Nutlin3a-treated $p21^{-/-}$ mice (Figure 2B), but it provided minor (albeit significant) protection against loss of mature T and B lymphocytes from lymph nodes (Figure S2C). This protection was,

(F and G) Cell-cycle analysis (F) and cell-survival analysis (G) after 12 hr of Nutlin3a treatment on mitogen-stimulated proliferating T lymphoblasts from mice of the indicated genotypes.

Cells were treated with 4 μM (D and E) or 10 μM (C, F, and G) Nutlin3a (or DMSO control), and cell viability and cell-cycle distribution were assessed by FACS. For (B)–(F), data represent mean ± SEM, from n = 3–4 mice per genotype. *$p < 0.05$.

See also Figure S1.

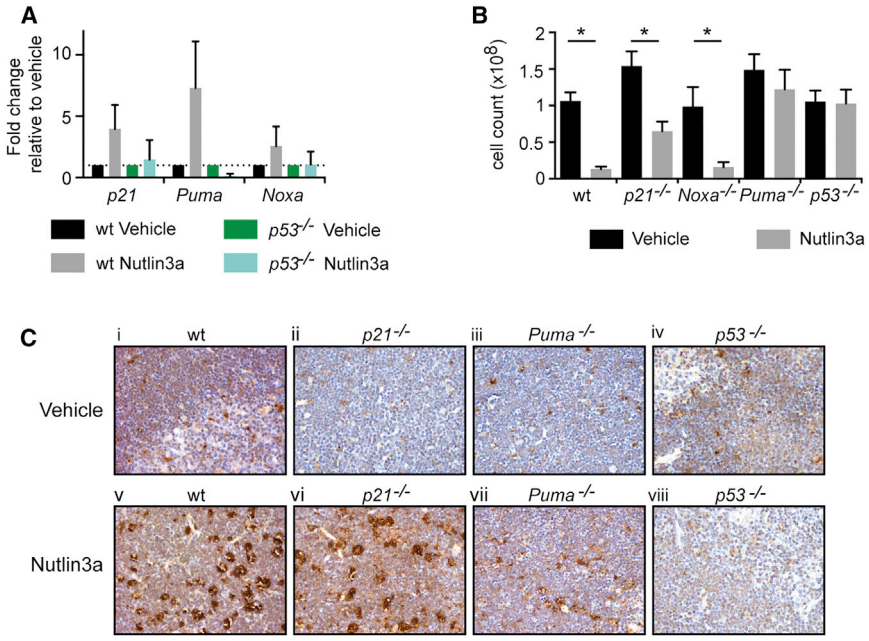

Figure 2. The BH3-Only Protein PUMA, but Not the CDKI p21, Is Critical for Nutlin3a-Induced, p53-Dependent Depletion of Thymocytes In Vivo

(A) Real-time qPCR analysis on thymi from mice 8 hr after one dose of Nutlin3a (200 mg/kg) or vehicle. Mean ± SEM from n = 3 mice per genotype (Figure S2B).

(B) Total Thy1$^+$CD4$^+$CD8$^+$ thymocyte numbers from mice of the indicated genotypes 24 hr after treatment with two doses of Nutlin3a (200 mg/kg) or vehicle. Mean ± SEM from n = 3–6 Nutlin3a/vehicle treatment pairs per genotype (Figure S2C). *$p < 0.05$.

(C) TUNEL staining on thymic sections from WT (i and v), *p53*$^{-/-}$ (iv and viii), *p21*$^{-/-}$ (ii and vi), and *Puma*$^{-/-}$ mice (iii and vii) that had been treated with vehicle (upper row) or Nutlin3a (200 mg/kg, lower row) for 8 hr; 3 Nutlin3a- and 3 vehicle-treated mice per genotype (Figure S2D).

See also Figures S2B–S2D.

however, considerably less than the complete protection provided by loss of PUMA or p53 (Figure S2C). Loss of NOXA did not provide resistance to Nutlin3a-induced depletion of thymocytes or mature T and B lymphocytes (Figure 2B; Figure S2C).

Histological TUNEL analysis (which reveals dsDNA breaks, a marker of apoptosis) showed that Nutlin3a treatment caused extensive alterations in the thymic architecture of WT mice, but not *p53*$^{-/-}$ mice, with extensive accumulation of TUNEL$^+$ cells, predominantly within the cortex (Figure 2C). Nutlin3a-treated *p21*$^{-/-}$ mice showed a similar increase in the numbers of TUNEL$^+$ cells in their thymi, as was seen in WT animals (Figure 2C). In contrast, thymi of Nutlin3a-treated *Puma*$^{-/-}$ mice contained only a few TUNEL$^+$ cells (Figure 2C). Large increases in the numbers of TUNEL$^+$ cells were also observed in the lymph nodes of WT and *p21*$^{-/-}$ mice, but not in those of *Puma*$^{-/-}$ or *p53*$^{-/-}$ mice (Figure S2D). The minor "protective" effect provided by the loss of p21 in the lymph nodes may, therefore, be due to failure to induce proliferative arrest after p53 activation rather than a direct effect on apoptosis. Notably, p21 has been shown to play a critical role in the inhibition of T cell proliferation after mitogen plus cytokine (concanavaline A [ConA] and interleukin-2 [IL-2]) stimulation (Balomenos et al., 2000). Collectively, these results demonstrate that losses of lymphoid cells induced by Nutlin3a in vitro and in vivo are primarily driven by PUMA-mediated apoptosis.

Malignant *Eμ-Myc* Lymphoma Cells Are Markedly More Sensitive to Nutlin3a Compared to Non-transformed Lymphoid Cells

To investigate the p53 effector processes critical for Nutlin3a's therapeutic effects on malignant cells, we utilized the *Eμ-Myc* transgenic mouse model (Adams et al., 1985). In these mice, deregulated MYC expression, found in ~70% of human cancers (Boxer and Dang, 2001), causes a pre-leukemic expansion of cycling pre-B cells, which, upon acquisition of cooperating oncogenic mutations, progress to clonal pre-B or sIg$^+$ B cell lymphomas (Adams et al., 1985).

Initially, we compared the sensitivity to Nutlin3a treatment in culture between pre-leukemic and malignant lymphoid cells from *Eμ-Myc* mice and their non-transformed WT counterparts. Both pre-leukemic *Eμ-Myc* pre-B and B cells and malignant *Eμ-Myc* lymphomas were markedly more sensitive to Nutlin3a than non-transformed mouse B lymphoid cells. This suggests that dysregulated MYC expression alone (and not the transformed state) sensitizes lymphoid cells to Nutlin3a-induced killing (Figure 3A). Notably, >90% of WT non-transformed B lymphoid cells remained viable after 4 hr of exposure to doses of Nutlin3a that were able to kill >70% of the pre-leukemic as well as malignant lymphoma cells from *Eμ-Myc* mice (Figure 3A). This suggests that it may be possible to define a therapeutic window for drugs that activate p53 via non-genotoxic processes in which malignant lymphoid cells are killed efficiently without inducing unacceptable losses of normal lymphoid (and other) cell types.

Nutlin3a Promotes p53 Accumulation and Downstream Effector Pathway Activation in *Eμ-Myc* Lymphoma Cells In Vitro

Western blot analysis revealed that Nutlin3a treatment promoted the accumulation of p53 protein within 4 hr, with co-incident increase of its downstream targets—PUMA and p21—in *Eμ-Myc* lymphoma-derived cell lines with confirmed WT p53 pathway activity, but not in *Eμ-Myc;p53*$^{-/-}$ lymphomas (Figure 3B; Figure S3A). Accordingly, real-time qPCR analysis demonstrated that Nutlin3a caused a p53-dependent increase in the levels of the p53 target genes, *Puma*, *Noxa*, *p21*, and *Mdm2*, in several independent *Eμ-Myc* lymphoma cell lines, but not in *Eμ-Myc; p53*$^{-/-}$ lymphoma cells (Figure 3C).

Low doses of Nutlin3a were sufficient to cause rapid apoptosis in *Eμ-Myc* lymphoma cell lines with WT p53, with 80%–90% cell

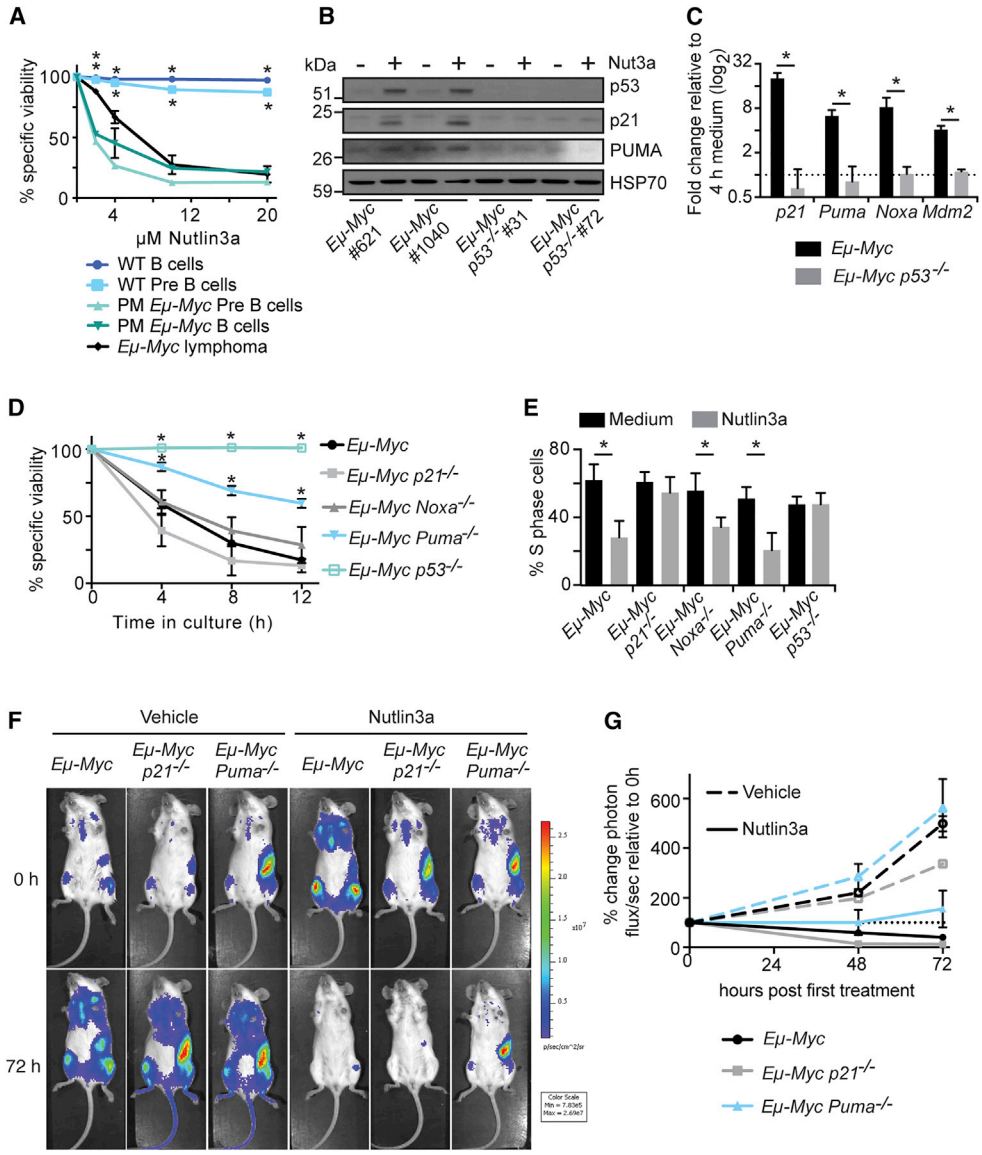

Figure 3. PUMA, but Not p21, Is Critical for Nutlin3a-Induced, p53-Dependent Killing In Vitro, and Regression In Vivo, of Malignant *Eμ-Myc* Lymphoma Cells

(A) Sorted primary B220^{+}IgM^{+} mature B cells (lymph node), B220^{+}IgM^{-} pre B cells (bone marrow) of WT or pre-malignant (PM) *Eμ-Myc* mice, and malignant *Eμ-Myc* lymphoma cells (with verified functional p53) were treated for 4 hr with 4–20 μM Nutlin3a or DMSO (control), and cell viability was assessed by FACS (Figure S3A). n = 3 mice per cell type (for pre-B and sIg^{+} B cells), and n = 5 for *Eμ-Myc* lymphoma cell lines, 3 independent experiments per cell line. *p < 0.05.

(B) Western blot analysis of *Eμ-Myc* and *Eμ-Myc;p53*$^{-/-}$ lymphoma-derived cell lines treated for 4 hr with 4 μM Nutlin3a or DMSO (control) in the presence of QVD-OPH (25 μM).

(C) Real-time qPCR analysis of *Eμ-Myc* and *Eμ-Myc;p53*$^{-/-}$ lymphoma cell lines treated for 4 hr with 4 μM Nutlin3a or DMSO (control) in the presence of QVD-OPH.

(D and E) Cell-survival (D) and cell-cycle (E) analysis of *Eμ-Myc* lymphoma cell lines of the indicated genotypes treated with Nutlin3a in vitro (Figure S3).

(F) In vivo live imaging of C57BL/6 albino mice transplanted with *Eμ-Myc* lymphoma cell lines of the indicated genotypes transduced with a lentiviral vector co-expressing luciferase and GFP. Mice were treated with Nutlin3a or vehicle for 3 days, and tumor growth was monitored, using live imaging of luciferase bioluminescence as a marker of tumor burden.

(G) Quantitation of tumor burden in mice bearing *Eμ-Myc* (black), *Eμ-Myc;p21*$^{-/-}$ (gray), or *Eμ-Myc;Puma*$^{-/-}$ (blue) lymphomas (transduced with a lentiviral vector co-expressing luciferase and GFP) treated with Nutlin3a (solid line) or vehicle (dashed line). Tumor burden was determined by the total photon flux per second emitted from a region of interest (ROI) drawn around the entire mouse. Data are expressed as percent change in photon flux compared to 0 hr. Mean ± SEM.

For (D) and (E), *Eμ-Myc* lymphoma cells were treated with 4 μM Nutlin3a or DMSO (control), and cell viability and cell-cycle distribution (at 8 hr) were assessed by FACS analysis. For (A) and (C)–(E), mean ± SEM, n = 3–5 cell lines per genotype, three independent experiments per cell line. *p < 0.05. For (F) and (G), n = 2 *Eμ-Myc* cell lines, 1 *Eμ-Myc;p21*$^{-/-}$ cell line, and 2 *Eμ-Myc;Puma*$^{-/-}$ cell lines, with n = 1 vehicle-treated and n = 2 Nutlin3a-treated mice per cell line.

See also Figure S3.

death after 12 hr, whereas <5% killing was seen in *Eμ-Myc;p53*$^{-/-}$ lymphoma cells (Figure 3D; Figure S3B). Prior to cell death, Nutlin3a induced cell-cycle arrest (60%–70% decreases in the proportions of S-phase cells) in *Eμ-Myc* but not in *Eμ-Myc;p53*$^{-/-}$ lymphoma cells (Figure 3E).

PUMA, but Not p21, Is Critical for Nutlin3a-Induced Killing of *Eμ-Myc* Lymphoma Cells In Vitro

Next, we utilized lymphoma-derived cell lines from *Eμ-Myc* mice, which had been crossed to mice lacking the p53 downstream targets PUMA, NOXA, or p21, and tested their response to Nutlin3a in culture. Although *Eμ-Myc;p21*$^{-/-}$ lymphoma lines did not undergo G1-S boundary cell-cycle arrest upon treatment with Nutlin3a, they were killed as efficiently as control *Eμ-Myc* cell lines (Figures 3D and 3E). In contrast, *Eμ-Myc;Puma*$^{-/-}$ lymphoma lines retained the ability to undergo cell-cycle arrest but were resistant to Nutlin3a-induced killing, with ~60% of cells remaining viable after 12 hr of treatment, when most (>95%) *Eμ-Myc*, *Eμ-Myc;p21*$^{-/-}$, and *Eμ-Myc;Noxa*$^{-/-}$ lymphoma cells had died (Figures 3D and 3E). Notably, there was a significant difference in viability between *Eμ-Myc;Puma*$^{-/-}$ and *Eμ-Myc;p53*$^{-/-}$ lymphoma lines, with the latter showing <5% killing after 12-hr Nutlin3a treatment (Figure 3D).

Loss of PUMA, but not Loss of p21, Impairs Regression of *Eμ-Myc* Lymphomas in Response to Nutlin3a In Vivo

Then, we transduced *Eμ-Myc* lymphoma lines with a lentiviral GFP-luciferase construct and transplanted them into non-irradiated C57BL/6 albino mice (Kelly et al., 2014). Once tumors were established, lymphoma-bearing mice were treated with Nutlin3a or vehicle twice daily for 3 days, and tumor growth was monitored using live imaging of luciferase bioluminescence.

All *Eμ-Myc* lymphomas tested progressed at a similar rate in the absence of Nutlin3a treatment (Figure 3F). In contrast, *Eμ-Myc* (control) lymphomas treated with Nutlin3a regressed substantially, with almost complete disappearance of the lymphoma (luciferase signal) observed after 72 hr of treatment (Figures 3F and 3G). Loss of p21 did not impair the therapeutic impact of Nutlin3a (Figures 3F and 3G). In striking contrast, *Eμ-Myc;Puma*$^{-/-}$ lymphomas were markedly resistant to Nutlin3a treatment, with mice bearing such lymphomas retaining a similar tumor burden when compared to pre-treatment values (Figures 3F and 3G). However, *Eμ-Myc;Puma*$^{-/-}$ lymphomas progressed more slowly in Nutlin3a-treated recipients, compared to their vehicle-treated controls, suggesting that, while PUMA-mediated apoptosis is critical for the regression of lymphoid malignancies in response to Nutlin3a treatment, this drug can impair lymphoma growth through additional processes (Figures 3F and 3G). It is, however, important to note that, in other tumors, such as solid cancers, p21-mediated growth arrest/senescence might contribute to the therapeutic impact of Nutlin3a. Indeed, previous studies showed that acute restoration of p53 in spontaneously arising sarcomas and mutant *HrasV12D*-driven murine liver carcinomas resulted in tumor regression in the absence of apoptosis, but with the appearance of markers of senescence (Martins et al., 2006; Ventura et al., 2007).

PUMA Contributes to Nutlin3a-Induced Apoptosis in Human Hematopoietic-Tumor-Derived Cell Lines In Vitro

Next, we tested whether PUMA is a critical determinant of Nutlin3a-induced killing of tumor cells in human neoplastic disease. We evaluated a panel of human hematopoietic-tumor-derived cell lines of different sub-types, including myeloid leukemia, multiple myeloma, and Burkitt lymphoma (Figure 4A), each of which with known *p53* status (Petitjean et al., 2007). Nutlin3a efficiently induced apoptosis in all cell lines tested with wild-type *p53*, but not in those harboring *p53* mutations, and this killing could be prevented by the caspase inhibitor QVD-OPH (Figure 4B; Figure S4). Nutlin3a treatment caused induction of TP53 protein, PUMA, and p21 in all WT p53 human hematopoietic-cancer-derived cell lines, but not in the *p53* mutated BL41 cell line (Figure 4C).

To test the contribution of PUMA to Nutlin3a-induced apoptosis, we used an inducible CRISPR/Cas9 platform to target the *PUMA* gene in our human cancer lines (Aubrey et al., 2015). Deletion of PUMA impaired induction of apoptosis in all three *p53* WT cell lines evaluated, as compared to the non-targeting small guide RNA (sgRNA) transduced control cells (Figure 4D). Given that the cell survival experiments were performed on a polyclonal population of cells, the gene deletion across the whole-cell population may not be complete; therefore, the protection likely represents an underestimate of the true impact of loss of PUMA. Efficient targeting of *PUMA* was confirmed by western blot analysis showing loss of induction of the WT PUMA protein, while induction of p53 protein and its target, p21, remained intact (Figure 4E). Taken together, these results indicate that PUMA-mediated apoptosis is a critical mediator of the therapeutic response of human hematopoietic cancer cells to Nutlin3a.

Interestingly, across multiple cellular contexts, and in both human and mouse cells, the protection from Nutlin3a-induced cell death afforded by loss of PUMA was not complete (Figures 1E, 3D, 3F, 3G, and 4D). This indicates that additional processes can contribute to Nutlin3a-induced tumor regression. The pro-apoptotic BH3-only protein BIM may be an interesting candidate, since the combined loss of BIM, along with PUMA and NOXA, fully protects *Eμ-Myc* lymphoma cells against DNA-damage-induced, p53-dependent killing (Happo et al., 2010) and since BIM loss provides non-transformed thymocytes with minor protection against etoposide (Bouillet et al., 1999; Erlacher et al., 2006). Since the *Bim* gene does not have an obvious p53-binding site (Bouillet et al., 2001), it may be activated indirectly by this tumor suppressor.

In conclusion, the results from this study demonstrate that induction of apoptosis by PUMA, but not induction of G1/S cell-cycle arrest by p21, is essential for p53-dependent Nutlin3a-induced killing of non-transformed murine lymphoid cells as well as malignant murine or human hematopoietic cells. Since a pro-apoptotic BH3-only protein, PUMA, is critical for the therapeutic impact of Nutlin3a, it may be possible to boost its therapeutic efficacy by the addition of BH3 mimetic drugs, such as ABT-263 (Navitoclax) or ABT-199, which inhibit BCL-2, BCL-XL plus BCL-W, or BCL-2 alone, respectively (Czabotar et al., 2014).

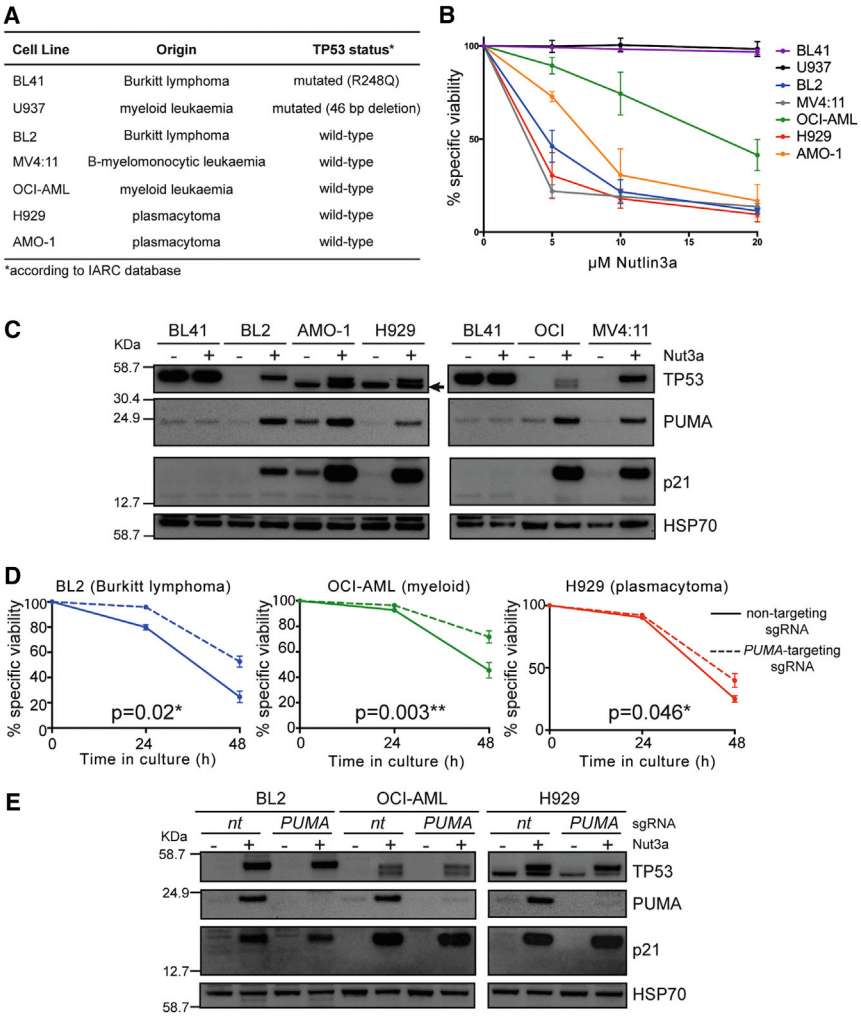

Figure 4. PUMA Contributes to Nutlin3a-Induced Killing of Human Hematopoietic-Cancer-Derived Cell Lines In Vitro

(A) Panel of selected human hematopoietic-cancer-derived cell lines with p53 status indicated, according to the International Agency for Research on Cancer (IARC) p53 database (Petitjean et al., 2007).

(B) Human cancer cell lines were treated with Nutlin3a for 48 hr at the indicated concentrations, and cell viability was assessed by FACS. Mean ± SEM from 3 independent experiments.

(C) Western blot analysis of human hematopoietic-tumor-derived cell lines after 24 hr treatment with 10 μM Nutlin3a. A cross-reacting protein (lower band) was detected by the antibody against human p53 in certain cell lines (arrow).

(D) Cell-survival analysis following Nutlin3a treatment of BL2 (10 μM), OCI-AML (20 μM), and H929 (10 μM) cell lines that had been transduced with either a non-targeting sgRNA (nt) (solid line) or a *PUMA*-targeting sgRNA (dashed line). Mean ± SEM; p values were derived from a paired two-tailed t test for n = 3 independent experiments at the 48-hr time point.

(E) Western blot analysis of Nutlin3a-treated CRISPR/Cas9 *PUMA*-targeted human cancer cell lines.

See also Figure S4.

EXPERIMENTAL PROCEDURES

Materials

Nutlin3a was provided by Roche Pharmaceuticals (Vassilev et al., 2004). For in vitro use, lyophilized Nutlin3a was dissolved in DMSO; for in vivo use, Nutlin3a was formulated in vehicle (2% Klucel, 0.5% Tween 80) and administered at 200 mg/kg body weight per dose by oral gavage twice daily for 1–3 days. For cells used for western blot or real-time qPCR analysis, 25 μM of the caspase inhibitor QVD-OPH (MP Biomedicals) was added 1 hr prior to the addition of cytotoxic drugs.

Mice

All experiments with mice followed the guidelines of the Melbourne Directorate Animal Ethics Committee. C57BL/6 mice were obtained from the Walter and Eliza Hall Institute's breeding facility. Generation and genotyping of mice deficient for p21 (Deng et al., 1995); NOXA, PUMA (Villunger et al., 2003); both PUMA and NOXA (Michalak et al., 2008); both PUMA and p21 (Valente et al., 2013); or p53 (Jacks et al., 1994) and *Eμ-Myc* transgenic mice (Adams et al., 1985) have been described. All mice were kept on a C57BL/6 background, generated either on this background using C57BL/6-derived embryonic stem (ES) cells (*Puma*$^{-/-}$ and *Noxa*$^{-/-}$) or on a mixed C57BL/6x129SV background using 129SV-derived ES cells and backcrossed with C57BL/6 mice for >12 generations (*p21*$^{-/-}$, *p53*$^{-/-}$). *Eμ-Myc* transgenic mice lacking BH3-only proteins were generated as described in the Supplemental Experimental Procedures.

Cell-Viability Assays

Non-transformed CD4^{+}CD8^{+} thymocytes; CD4^{+} and CD8^{+} T lymphocytes; and B220^{+}sIg^{-} pre-B and B220^{+}sIg^{+} mature B cells were FACS sorted from the thymus, lymph nodes, and bone marrow, respectively. Non-transformed lymphoid cells, *Eμ-Myc* lymphoma cell lines, and human hematopoietic cancer cell lines were treated with the indicated concentrations of compound, and cell viability was assessed by FACS after staining with fluorescein isothiocyanate (FITC)-conjugated Annexin V plus propidium iodide (PI; 2 μg/ml, Sigma); note that, for human cancer cell lines, PI alone was used to assess cell viability. Cell viability was expressed as percent Annexin-V^{negative}PI^{negative} cells (or PI^{negative} for human cells) relative to untreated controls.

Cell-Cycle Analysis

Mitogen-stimulated T cell lymphoblasts were generated as described in the Supplemental Experimental Procedures. Proliferating T cells and *Eμ-Myc* lymphoma lines were treated with the indicated concentrations of Nutlin3a or DMSO (control). Cell-cycle distribution was assessed by PI staining and FACS analysis (Riccardi and Nicoletti, 2006).

Western Blot and Real-Time qPCR Analyses

Total cell protein extracts were prepared in either ONYX or RIPA buffer, supplemented with complete protease inhibitor cocktail (Roche). The antibodies listed here in parentheses were used to detect the following proteins: for detection of mouse proteins, p21 (C-19; Santa Cruz Biotechnology); p53 (CM5; Novacastra); PUMA (ab27669; Abcam); MDM2 (sc812; Santa Cruz Biotech); and p19ARF (5.C3.1; Rockland Antibodies and Assays). For detection of human proteins: p21 (ab7960; Abcam); p53 (FL-393) (sc-6243; Santa Cruz Biotechnology); PUMA (ab27669, Abcam); and HSP70 (both mouse and human, clone N6; a gift from Dr. R. Anderson, Peter MacCallum Cancer Research Institute).

Total RNA was isolated from cells using TRIzol (Invitrogen) and reverse transcribed using SuperScript II Reverse Transcriptase (Invitrogen) and Oligo-d(T)

primers. Real-time qPCR was performed in triplicate using Taqman Gene Expression assays (Applied Biosystems) and an ABI 7900 Real-Time PCR Machine (Applied Biosystems). mRNA expression levels were standardized by comparison to the transcript levels of the reference gene, *Hmbs*, based on the comparative threshold method (DD_{Ct}).

In Vivo Treatment Studies

Age-matched mice were treated for 1 day (two doses) with 200 mg/kg body weight Nutlin3a or vehicle. Total organ cell counts were determined, and leukocyte subset distribution was determined as described previously (Strasser et al., 1991) by FACS analysis after staining with surface-marker-specific monoclonal antibodies that had been coupled to FITC, R-phycoerythrin (R-PE), or allophycocyanin (APC). From this, total cell population counts were calculated.

Eμ-Myc lymphoma-derived cell lines were transduced with a lentiviral FUL2tG expression construct (driving co-expression of GFP and luciferase) (Kelly et al., 2014). Cells transduced with the construct (GFP^+) were sorted, and 1×10^6 cells (in 200 μl PBS) injected intravenously (i.v.) into C57BL/6 albino recipient mice. Tumor growth was monitored by live imaging using the IVIS Spectrum In Vivo Imaging System (PerkinElmer) to detect luciferase bioluminescence. When lymphoma burden was sufficiently high (~7 days post-injection, photon flux per second of $>1 \times 10^8$), mice were treated with 200 mg/kg body weight Nutlin3a or vehicle twice daily for 3 days, and tumor growth was monitored at the indicated time points.

Histology and TUNEL Staining

Organs from Nutlin3a- or vehicle-treated mice were harvested at 8 hr and fixed in 10% formalin prior to sectioning. TUNEL staining was performed as previously described (Michalak et al., 2008).

CRISPR/Cas9-Mediated *PUMA* Gene Disruption

PUMA knockout cell lines were generated using a previously described inducible lentiviral CRISPR/Cas9 platform (Aubrey et al., 2015). Lentivirus was produced using packaging constructs pRSV-rev, pMDL, and pVSV-G, as previously described (Aubrey et al., 2015). We used inducible sgRNAs targeting exon 3 (5′- GCCGCTCGTACTGTGCGTTG-3′) of the *PUMA* gene or a non-targeting sgRNA (5′-GACAATTGCAGCCTGCTGAG-3′). Stable, constitutive, lentivirus-mediated Cas9 expression, reported by mCherry fluorescent protein expression, was achieved as previously described (Aubrey et al., 2015). Inducible sgRNA lentiviral vectors were used, and their presence was reported by EGFP expression. mCherry and eGFP double-positive cells were isolated using FACS sorting in an Influx flow cytometer (Becton Dickinson). Whole-cell populations were treated for 1 week with doxycycline hyclate (Sigma-Aldrich, D9891), at a final concentration of 1 μg/ml to induce expression of the *PUMA*-targeting or non-targeting control sgRNA. To confirm correct *PUMA* gene targeting, selected samples were assessed using the MiSeq Indel sequencing platform as previously described (Aubrey et al., 2015) (data not shown).

Statistical Analysis

Prism (Version 5; GraphPad) software was used for all statistical analyses. Two-group comparisons were made using two-tailed Student's t tests assuming equal variances. Comparisons between multiple groups were made using One-way ANOVA (Tukey's multiple comparison test/Kruskal-Wallis test). p values < 0.05 were considered to indicate statistical significance.

SUPPLEMENTAL INFORMATION

Supplemental Information includes Supplemental Experimental Procedures and four figures and can be found with this article online at http://dx.doi.org/10.1016/j.celrep.2016.01.059.

AUTHOR CONTRIBUTIONS

L.J.V., B.J.A., L.T.V., and A.S. conceived the study, planned experiments, and interpreted results. L.J.V., and B.J.A. conducted the experiments. L.J.V., B.J.A., and A.S. prepared, reviewed, and edited the manuscript. M.J.H., G.L.K., L.H., C.L.S., A.N., R.W.J., D.C.S.H., and L.T.V. provided advice and reagents for experiments.

ACKNOWLEDGMENTS

We thank Drs. J.M. Adams, A. Villunger, P. Bouillet, and S. Cory for gifts of mice; Drs. D. Segal, S. Glaser, and Y. Yao for human cancer cell lines; G. Siciliano and his colleagues for animal husbandry; E. Tsui and her colleagues for help with histology; S. Monard and his team for help with flow cytometry; Drs. S. Wilcox and A. Kueh for MiSeq runs and assistance with sample preparation; and Dr. L. Rohrbeck for the *PUMA* sgRNA and MiSeq primers. Work in the authors' laboratories was supported by the National Health and Medical Research Council (NHMRC) of Australia (program grant 1016701, project grants 1046010 and 637326, and fellowship #1020363); the Leukemia and Lymphoma Society (SCOR grant #7413); the Cancer Council Victoria (post-graduate research fellowship to L.J.V.; project grant 1052309 to A.S.; Sir Edward Dunlop Fellowship in Cancer Research to C.L.S.); the Leukaemia Foundation National Research Program Clinical PhD Scholarship (to B.J.A.); and the Victorian Cancer Agency (clinical fellowship to C.L.S.). R.W.J. is a Principal Research Fellow of the NHMRC of Australia and supported by NHMRC program and project grants and by the Cancer Council Victoria. This work was made possible by operational infrastructure grants through the Australian Government (IRISS), the Victorian State Government (OIS), and the Australian Cancer Research Foundation.

Received: February 19, 2014
Revised: November 23, 2015
Accepted: January 16, 2016
Published: February 18, 2016

REFERENCES

Adams, J.M., Harris, A.W., Pinkert, C.A., Corcoran, L.M., Alexander, W.S., Cory, S., Palmiter, R.D., and Brinster, R.L. (1985). The c-*myc* oncogene driven by immunoglobulin enhancers induces lymphoid malignancy in transgenic mice. Nature *318*, 533–538.

Aubrey, B.J., Kelly, G.L., Kueh, A.J., Brennan, M.S., O'Connor, L., Milla, L., Wilcox, S., Tai, L., Strasser, A., and Herold, M.J. (2015). An inducible lentiviral guide RNA platform enables the identification of tumor-essential genes and tumor-promoting mutations in vivo. Cell Rep. *10*, 1422–1432.

Balomenos, D., Martín-Caballero, J., García, M.I., Prieto, I., Flores, J.M., Serrano, M., and Martínez-A, C. (2000). The cell cycle inhibitor p21 controls T-cell proliferation and sex-linked lupus development. Nat. Med. *6*, 171–176.

Bouillet, P., Metcalf, D., Huang, D.C.S., Tarlinton, D.M., Kay, T.W.H., Köntgen, F., Adams, J.M., and Strasser, A. (1999). Proapoptotic Bcl-2 relative Bim required for certain apoptotic responses, leukocyte homeostasis, and to preclude autoimmunity. Science *286*, 1735–1738.

Bouillet, P., Zhang, L.C., Huang, D.C., Webb, G.C., Bottema, C.D., Shore, P., Eyre, H.J., Sutherland, G.R., and Adams, J.M. (2001). Gene structure alternative splicing, and chromosomal localization of pro-apoptotic Bcl-2 relative Bim. Mamm. Genome *12*, 163–168.

Boxer, L.M., and Dang, C.V. (2001). Translocations involving c-*myc* and c-*myc* function. Oncogene *20*, 5595–5610.

Brugarolas, J., Chandrasekaran, C., Gordon, J.I., Beach, D., Jacks, T., and Hannon, G.J. (1995). Radiation-induced cell cycle arrest compromised by p21 deficiency. Nature *377*, 552–557.

Chang, B.D., Xuan, Y., Broude, E.V., Zhu, H., Schott, B., Fang, J., and Roninson, I.B. (1999). Role of p53 and p21waf1/cip1 in senescence-like terminal proliferation arrest induced in human tumor cells by chemotherapeutic drugs. Oncogene *18*, 4808–4818.

Czabotar, P.E., Lessene, G., Strasser, A., and Adams, J.M. (2014). Control of apoptosis by the BCL-2 protein family: implications for physiology and therapy. Nat. Rev. Mol. Cell Biol. *15*, 49–63.

Deng, C., Zhang, P., Harper, J.W., Elledge, S.J., and Leder, P. (1995). Mice lacking p21CIP1/WAF1 undergo normal development, but are defective in G1 checkpoint control. Cell *82*, 675–684.

Efeyan, A., Ortega-Molina, A., Velasco-Miguel, S., Herranz, D., Vassilev, L.T., and Serrano, M. (2007). Induction of p53-dependent senescence by the MDM2 antagonist nutlin-3a in mouse cells of fibroblast origin. Cancer Res. *67*, 7350–7357.

Erlacher, M., Labi, V., Manzl, C., Böck, G., Tzankov, A., Häcker, G., Michalak, E., Strasser, A., and Villunger, A. (2006). Puma cooperates with Bim, the rate-limiting BH3-only protein in cell death during lymphocyte development, in apoptosis induction. J. Exp. Med. *203*, 2939–2951.

Freedman, D.A., Wu, L., and Levine, A.J. (1999). Functions of the MDM2 oncoprotein. Cell. Mol. Life Sci. *55*, 96–107.

Gartel, A.L., and Tyner, A.L. (2002). The role of the cyclin-dependent kinase inhibitor p21 in apoptosis. Mol. Cancer Ther. *1*, 639–649.

Happo, L., Cragg, M.S., Phipson, B., Haga, J.M., Jansen, E.S., Herold, M.J., Dewson, G., Michalak, E.M., Vandenberg, C.J., Smyth, G.K., et al. (2010). Maximal killing of lymphoma cells by DNA damage-inducing therapy requires not only the p53 targets Puma and Noxa, but also Bim. Blood *116*, 5256–5267.

Jacks, T., Remington, L., Williams, B.O., Schmitt, E.M., Halachmi, S., Bronson, R.T., and Weinberg, R.A. (1994). Tumor spectrum analysis in *p53*-mutant mice. Curr. Biol. *4*, 1–7.

Jänicke, R.U., Sohn, D., Essmann, F., and Schulze-Osthoff, K. (2007). The multiple battles fought by anti-apoptotic p21. Cell Cycle *6*, 407–413.

Jeffers, J.R., Parganas, E., Lee, Y., Yang, C., Wang, J., Brennan, J., MacLean, K.H., Han, J., Chittenden, T., Ihle, J.N., et al. (2003). Puma is an essential mediator of p53-dependent and -independent apoptotic pathways. Cancer Cell *4*, 321–328.

Kelly, G.L., Grabow, S., Glaser, S.P., Fitzsimmons, L., Aubrey, B.J., Okamoto, T., Valente, L.J., Robati, M., Tai, L., Fairlie, W.D., et al. (2014). Targeting of MCL-1 kills MYC-driven mouse and human lymphomas even when they bear mutations in p53. Genes Dev. *28*, 58–70.

Kerr, J.B., Hutt, K.J., Cook, M., Speed, T.P., Strasser, A., Findlay, J.K., and Scott, C.L. (2012). Cisplatin-induced primordial follicle oocyte killing and loss of fertility are not prevented by imatinib. Nat. Med. *18*, 1170–1172, author reply, 1172–1174.

Martins, C.P., Brown-Swigart, L., and Evan, G.I. (2006). Modeling the therapeutic efficacy of p53 restoration in tumors. Cell *127*, 1323–1334.

Michalak, E.M., Villunger, A., Adams, J.M., and Strasser, A. (2008). In several cell types tumour suppressor p53 induces apoptosis largely via Puma but Noxa can contribute. Cell Death Differ. *15*, 1019–1029.

Momand, J., Jung, D., Wilczynski, S., and Niland, J. (1998). The MDM2 gene amplification database. Nucleic Acids Res. *26*, 3453–3459.

Oda, E., Ohki, R., Murasawa, H., Nemoto, J., Shibue, T., Yamashita, T., Tokino, T., Taniguchi, T., and Tanaka, N. (2000). Noxa, a BH3-only member of the Bcl-2 family and candidate mediator of p53-induced apoptosis. Science *288*, 1053–1058.

Ogilvy, S., Metcalf, D., Print, C.G., Bath, M.L., Harris, A.W., and Adams, J.M. (1999). Constitutive Bcl-2 expression throughout the hematopoietic compartment affects multiple lineages and enhances progenitor cell survival. Proc. Natl. Acad. Sci. USA *96*, 14943–14948.

Petitjean, A., Mathe, E., Kato, S., Ishioka, C., Tavtigian, S.V., Hainaut, P., and Olivier, M. (2007). Impact of mutant p53 functional properties on TP53 mutation patterns and tumor phenotype: lessons from recent developments in the IARC TP53 database. Hum. Mutat. *28*, 622–629.

Riccardi, C., and Nicoletti, I. (2006). Analysis of apoptosis by propidium iodide staining and flow cytometry. Nat. Protoc. *1*, 1458–1461.

Rigatti, M.J., Verma, R., Belinsky, G.S., Rosenberg, D.W., and Giardina, C. (2012). Pharmacological inhibition of Mdm2 triggers growth arrest and promotes DNA breakage in mouse colon tumors and human colon cancer cells. Mol. Carcinog. *51*, 363–378.

Riley, T., Sontag, E., Chen, P., and Levine, A. (2008). Transcriptional control of human p53-regulated genes. Nat. Rev. Mol. Cell Biol. *9*, 402–412.

Shibue, T., Takeda, K., Oda, E., Tanaka, H., Murasawa, H., Takaoka, A., Morishita, Y., Akira, S., Taniguchi, T., and Tanaka, N. (2003). Integral role of Noxa in p53-mediated apoptotic response. Genes Dev. *17*, 2233–2238.

Strasser, A., Harris, A.W., and Cory, S. (1991). *bcl-2* transgene inhibits T cell death and perturbs thymic self-censorship. Cell *67*, 889–899.

Tian, H., Wittmack, E.K., and Jorgensen, T.J. (2000). p21WAF1/CIP1 antisense therapy radiosensitizes human colon cancer by converting growth arrest to apoptosis. Cancer Res. *60*, 679–684.

Tovar, C., Rosinski, J., Filipovic, Z., Higgins, B., Kolinsky, K., Hilton, H., Zhao, X., Vu, B.T., Qing, W., Packman, K., et al. (2006). Small-molecule MDM2 antagonists reveal aberrant p53 signaling in cancer: implications for therapy. Proc. Natl. Acad. Sci. USA *103*, 1888–1893.

Valente, L.J., Gray, D.H., Michalak, E.M., Pinon-Hofbauer, J., Egle, A., Scott, C.L., Janic, A., and Strasser, A. (2013). p53 efficiently suppresses tumor development in the complete absence of its cell-cycle inhibitory and proapoptotic effectors p21, Puma, and Noxa. Cell Rep. *3*, 1339–1345.

Valentine, J.M., Kumar, S., and Moumen, A. (2011). A p53-independent role for the MDM2 antagonist Nutlin-3 in DNA damage response initiation. BMC Cancer *11*, 79.

Vassilev, L.T., Vu, B.T., Graves, B., Carvajal, D., Podlaski, F., Filipovic, Z., Kong, N., Kammlott, U., Lukacs, C., Klein, C., et al. (2004). In vivo activation of the p53 pathway by small-molecule antagonists of MDM2. Science *303*, 844–848.

Ventura, A., Kirsch, D.G., McLaughlin, M.E., Tuveson, D.A., Grimm, J., Lintault, L., Newman, J., Reczek, E.E., Weissleder, R., and Jacks, T. (2007). Restoration of p53 function leads to tumour regression in vivo. Nature *445*, 661–665.

Verma, R., Rigatti, M.J., Belinsky, G.S., Godman, C.A., and Giardina, C. (2010). DNA damage response to the Mdm2 inhibitor nutlin-3. Biochem. Pharmacol. *79*, 565–574.

Villunger, A., Michalak, E.M., Coultas, L., Müllauer, F., Böck, G., Ausserlechner, M.J., Adams, J.M., and Strasser, A. (2003). p53- and drug-induced apoptotic responses mediated by BH3-only proteins puma and noxa. Science *302*, 1036–1038.

Vogelstein, B., Lane, D., and Levine, A.J. (2000). Surfing the p53 network. Nature *408*, 307–310.

Xia, M., Knezevic, D., and Vassilev, L.T. (2011). p21 does not protect cancer cells from apoptosis induced by nongenotoxic p53 activation. Oncogene *30*, 346–355.

Xue, W., Zender, L., Miething, C., Dickins, R.A., Hernando, E., Krizhanovsky, V., Cordon-Cardo, C., and Lowe, S.W. (2007). Senescence and tumour clearance is triggered by p53 restoration in murine liver carcinomas. Nature *445*, 656–660.

University Library

MINERVA ACCESS

A gateway to Melbourne's research publications

Minerva Access is the Institutional Repository of The University of Melbourne

Author/s:
Valente, LJ; Aubrey, BJ; Herold, MJ; Kelly, GL; Happo, L; Scott, CL; Newbold, A; Johnstone, RW; Huang, DCS; Vassilev, LT; Strasser, A

Title:
Therapeutic Response to Non-genotoxic Activation of p53 by Nutlin3a Is Driven by PUMA-Mediated Apoptosis in Lymphoma Cells

Date:
2016-03-01

Citation:
Valente, L. J., Aubrey, B. J., Herold, M. J., Kelly, G. L., Happo, L., Scott, C. L., Newbold, A., Johnstone, R. W., Huang, D. C. S., Vassilev, L. T. & Strasser, A. (2016). Therapeutic Response to Non-genotoxic Activation of p53 by Nutlin3a Is Driven by PUMA-Mediated Apoptosis in Lymphoma Cells. CELL REPORTS, 14 (8), pp.1858-1866. https://doi.org/10.1016/j.celrep.2016.01.059.

Persistent Link:
http://hdl.handle.net/11343/113707

File Description:
Published version